PCCP

Accepted Manuscript

ROYAL SOCIETY OF CHEMISTRY

www.rsc.org/pccp

Physical Chemistry Chemical Physics

PAPER

Emission of highly excited electronic states of potassium from cryptomelane nanorods

Received 00th January 20xx,
Accepted 00th January 20xx

DOI: 10.1039/x0xx00000x

www.rsc.org/

P. Stelmachowski,[a] P. Legutko,[a] T. Jakubek,[a] P. Indyka,[a] Z. Sojka,[a] L. Holmlid[b] and A. Kotarba*[a]

Cryptomelane (KMn_8O_{16}) nanorods were synthesized, characterized (XRD, Raman spectroscopy, TEM/SAED) and investigated by species resolved thermal desorption of potassium from the material in the range of 20-620°C. The desorbing fluxes of ions, atoms and highly electronic excited states (field ionizable Rydberg states) were measured with ion collector, surface ionization and field ionization detectors, respectively, in a vacuum apparatus. The non-equilibrium emission of potassium Rydberg species (principal quantum number > 30) strongly depends on surface positive voltage bias with a broad maximum at 1 ÷ 8 V. The stimulation of Rydberg species emission is discussed in terms of spatial and energetic overlapping between the electron cloud above the cryptomelane surface and potassium ion desorption.

Introduction

Metal oxides are extensively used as heterogeneous catalysts in many various chemical reactions. Their promotion with alkali has proven to be an effective way to improve the most important parameters of catalytic performance, i.e., activity, selectivity and stability [1, 2, 3, 4]. Although alkali promotion is widely applied in practice, the detailed mechanism of the alkali effects is not well understood. This is due to high complexity of the catalytic systems and the diversity of the effects caused by the alkali addition. In general, the alkali addition may lead to either surface or bulk promotion. In the case of the latter, several phases have been intensively studied for possible catalytic applications, e.g. potassium ferrites in ethylbenzene dehydrogenation [5], alkali titanates for photocatalysis [6] or alkali manganates in soot oxidation [7].

Nanoscale alkali doped manganese octahedral molecular sieves (OMS's) are widely recognized as exceptional catalysts in total oxidation reactions [7, 8, 9, 10, 11]. Their high reactivity is attributed to a combination of several features including their beneficial porous structure, redox properties arising from mixed valence framework and high oxygen mobility [12, 13, 14]. Cryptomelane is a hollandite type manganese oxide with a tunnelled structure (OMS-2) nanostructured by alkali [15]. The tunnels are built up of four double-wide (2 x 2) slabs of octahedral MnO_6 units, which are connected by edges, resulting in the tunnel dimensions of 4.6x4.6 Å [16].

To explain the changes in catalysts activity resulting from alkali promotion, several mechanisms have been proposed including the modification of density of states/Fermi level characteristics, donor-acceptor energy levels or electrostatic interactions. For some potassium doped catalysts the promotional effect was suggested to originate from electronically excited states of alkali atoms, especially long-lived Rydberg states [17]. Due to their specific properties Rydberg states are considered to play a unique role in catalytic reactions [18] as a electrodonor species of extremely high cross section area.

Atoms or molecules are in a Rydberg state when one or more of their electrons have been excited to a high principal quantum number (n > 10-100), resulting in a large electronic orbit when compared to the size of the ground state atom. Several Rydberg states with circular electronic orbits may condense into Rydberg Matter (RM) when aligned planarly. Identical excitation levels and the coherent motion of the electrons are prerequisites for this process. Such clusters have very long lifetimes [19] and were found to be form during desorption from surfaces [14]. Indeed, RM has been observed on several potassium-loaded catalysts such as transition metal carbides and nitrates [20], graphite [21] and zirconia [22], as well as on noble metal surfaces [23]. Rydberg states of alkali metals have been studied experimentally for many years [24, 25] due to their interesting properties – thermally stimulated emission [26], strong long-range interactions [25] and relevance to catalytic activity [27]. Among the theoretical accounts, quantum defect model is usually used to describe a strongly non-Born–Oppenheimer behaviour of the Rydberg states [28,29].

In this work, we report on the emission of highly excited electronic states of potassium from a catalytically active phase of cryptomelane of nanorods morphology.

[a] Faculty of Chemistry, Jagiellonian University, ul. Ingardena 3, 30-060 Krakow, Poland.
*E-mail: kotarba@chemia.uj.edu.pl
[b] Department of Chemistry and Molecular Biology, University of Gothenburg, Göteborg, 412 96, Sweden.

Experimental

Synthesis

The reflux method was used to obtain the cryptomelane phase according to [7]. Briefly, 11 g of $Mn(CH_3COO)_2$ was dissolved in 40 ml of distilled water and the pH was adjusted to 5 by adding glacial acetic acid. The solution was heated to the boiling temperature under reflux and maintained for 45 min. 6.5 g of potassium permanganate was dissolved in 150 ml distilled water and added to the previously prepared Mn(II) acid solution and kept under reflux by energetic stirring for 24 h. The solid was filtered, washed with distilled water until neutral pH and dried at 120°C overnight. Finally, the product was calcined in air at 450°C for 2 h.

Physicochemical characterization

XRD patterns were recorded by a Rigaku MiniFlex powder diffractometer with Cu Kα radiation, 2θ step scans of 0.02° and a counting time of 1 s per step. The micro-Raman spectra were recorded in ambient conditions using a Renishaw InVia spectrometer equipped with a Leica DMLM confocal microscope and a CCD detector, with an excitation wavelength of 785 nm. The X-ray photoelectron spectra (XPS) were measured with a Prevac photoelectron spectrometer equipped with a hemispherical VG SCIENTA R3000 analyzer. The spectra were recorded using a monochromatized aluminum AlKα source (E = 1486.6 eV) and an electron flood gun (FS40A-PS). Microscopic images were acquired with a high resolution analytical transmission electron microscopy (FEI Tecnai Osiris) with X-FEG Schottky field emitter operated at accelerating voltage of 200 kV electron beam.

Microscopic characterization

Particle size and morphology were characterized using a high resolution transmission electron microscope (FEI Tecnai Osiris) with X-FEG Schottky field emitter operated at accelerating voltage of 200 kV. Powder samples were dispersed in ethanol, ultrasonicated, dropped into a lacey carbon-coated copper grid then dried at room temperature.

Alkali desorption experiments

The potassium thermal desorption experiments were carried out in a vacuum apparatus with a background pressure of 10^{-7} mbar. The samples were heated stepwise from room temperature to 620°C with a c.a. 10°C/step (0.5 V/step). The desorbing fluxes of potassium in form of atoms, ions and excited matter were measured. The atomic flux was determined with a surface ionization detector, as described in [30], in which the platinum filament was heated with the applied current of 2.2 A (1.7 V). Due to a low ionization potential, under such conditions, only potassium atoms were surface ionized. A positive potential of 120 V was applied to the filament to repel potassium desorbing in the form of ions. The positive voltage of 5 V was also applied to the sample to prevent electron emission. The ionic flux was determined with a plate collector and measured directly as an ionic current, which provided a high signal level. During this measurement a positive potential of 90 V was applied to the sample to accelerate potassium ions formed at the sample surface toward the detector. The excited potassium states were measured at a constant temperature with a field ionization detector as described in [31]. Two electrodes between the sample and the collector were held at +150 and –165 V, respectively, to obtain an electric field between the electrodes, which ionizes the excited alkali species. The field strength was 550 V/cm in the present case. In order to detect positive ions both electrodes were grounded and the positive bias voltage on the sample was changed in the range of 0-36 V. A positive signal was then measured at the collector. In all measurements, the positive current was measured directly with a digital electrometer Keithley 6512.

Results and discussion

The materials phase composition was verified by X-ray diffraction and Raman Spectroscopy measurements (Fig. 1A). The TEM microstructure characterization of investigated cryptomelane confirms its purity, crystallinity and well-ordered fibre–like morphology [32, 33, 34]. The diffraction lines, indexed using ICSD base (59159-ICSD), manifest the presence of only the cryptomelane phase. The calculated crystal size values based on the observed XRD line broadening (derived from the Scherrer formula) were found to be in the 9-22 nm range, which is in accordance with the TEM results presented below.

As shown in Fig.. 1 B the Raman scattering spectrum features four main contributions (183, 386, 574, and 634 cm^{-1}) and five weak bands (286, 330, 470, 512, and 753 cm^{-1}) as previously reported in [35]. The well-defined spectrum indicates the sample is of good crystallinity, which is in line with the structural studies presented. Following Gao et al. it can be interpreted noting that the

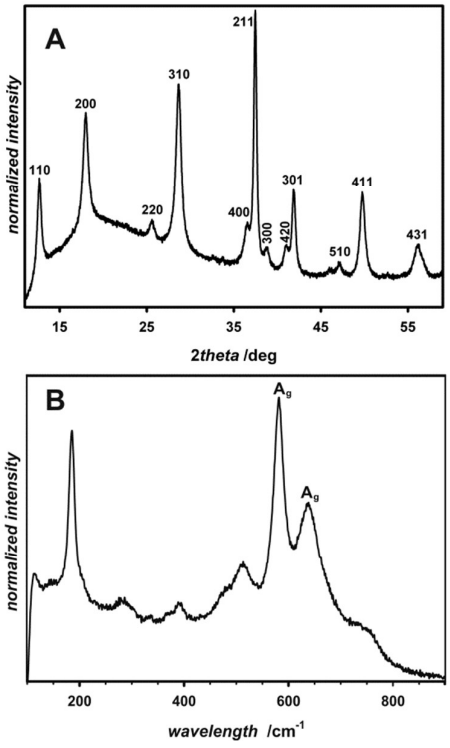

Fig. 1 A) Diffraction pattern and B) Raman spectrum of synthesized K-cryptomelane.

manganese atoms are five times heavier than oxygen atoms. Therefore, it is expected that the Mn–O vibrations mainly involve the displacement of the oxygen atoms. The two intense bands at 574 and 634 cm^{-1} may be thus assigned to the A_g symmetry species, and the vibration of Mn–O is indicative of a well-developed tetragonal structure with the 2 x 2 tunnels. The MnO_6 octahedra are connected via edges, hence the main vibrational interactions may be found along or perpendicular to the O–Mn–O–Mn–O chains. The presence of heavy cations inside the tunnel affects the vibrational components directed at the interior of the tunnel as can be seen by the changes of the intensity in the Raman band at 634 cm^{-1} when the cations are replaced. This band is therefore most likely related to a Mn–O vibration perpendicular to the direction of the octahedral chains. The Raman band at 574 cm^{-1} is believed to be related to the displacement of oxygen atoms relative to the manganese atoms along the octahedral chain. The low frequency Raman bands at 183, 386 and 753 cm^{-1} were assigned to an external vibration that derives from the translational motion of the MnO_6 octahedra, Mn–O bending vibrations and antisymmetric Mn–O stretching vibrations, respectively. The remaining Raman bands are also thought to be attributed to other Mn–O lattice vibrations.

TEM images revealed that the as-prepared sample comprised of isolated nanorod-shaped particles with pyramidal tip endings of the average length of about 500 nm and 20 nm in width (Fig. 2). Some of the individual cryptomelane particles were found agglomerated to each other along long axis <100> growth direction. Selected area electron diffraction (SAED) pattern taken from a large group of the nanorods consisted of concentric rings that can be indexed in accordance with the KMn_8O_{16} tetragonal structure. High aspect ratio of the nanorod morphology resulted in visible radial reflexion elongation in the electron diffraction pattern. High resolution TEM image revealed lattice fringes indicating preservation of a crystalline character of particles. Lattice distortions indicated the presence of dislocation defects along nanorod in the preferred growth direction.

The thermal desorption of alkali atoms and ions was found to begin in the 430-460°C range, that is comparable to other potassium-promoted materials [30, 36]. As presented in Fig. 3, the Arrhenius-like plot of K^+ thermal desorption exhibits a distinct linear character (correlation coefficient higher than 0.99) in the regions specified

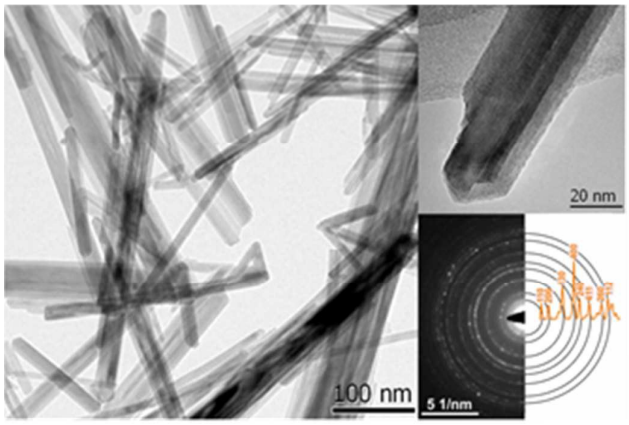

Fig. 2 TEM overview image of as-synthesized cryptomelane manganese oxide with the corresponding SAED pattern and nanorod HRTEM image.

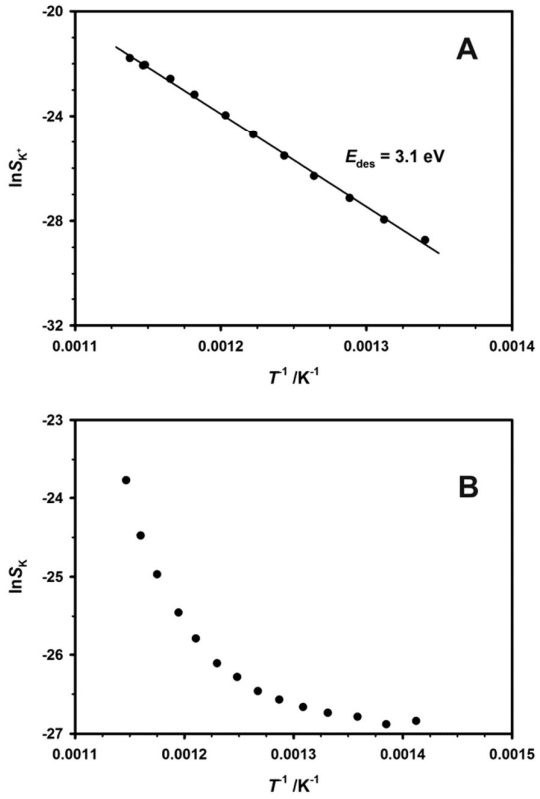

Fig. 3 Arrhenius type dependence of the desorption signal of potassium A) cations and B) atoms.

with the filled points. The activation energy for ion desorption was thus determined reliably (3.1± 0.1 eV). This value was previously fund to be typical for $K–O_{surf}$ for metal oxide surfaces [37]. On the other hand the potassium atom desorption proceeds in an exponential fashion, suggesting a secondary process such as Rydberg state desorption and the curve of the plot does not allow for direct activation energy calculation. It is also possible that this behaviour is due to cluster formation of the desorbing Rydberg atoms, as reported in [22, 38].

The thermal behaviour of potassium in the cryptomelane phase and especially on its surface is proposed to involve the formation of electronically excited states on the surface. Such states are formed during the emission of K^+ ions from the bulk due to the tunnelled structure of cryptomelane, which form fast diffusion pathways. The excited states are proposed to form at the cryptomelane surface thermally but in non-equilibrium concentrations. During the thermal desorption process, when the potassium-surface bond is broken, an electron from the low work function cryptomelane surface may be picked up to form so-called highly excited Rydberg states. These states, due to their large cross sections for reaction and facile electron transfer, may easily promote the reactivity of most reactants (R) approaching the surface and form K*–R or K–R* intermediates. Therefore, it is not surprising that a correlation between and activity and Rydberg state emission for various catalytic processes was observed, as revealed elsewhere [17].

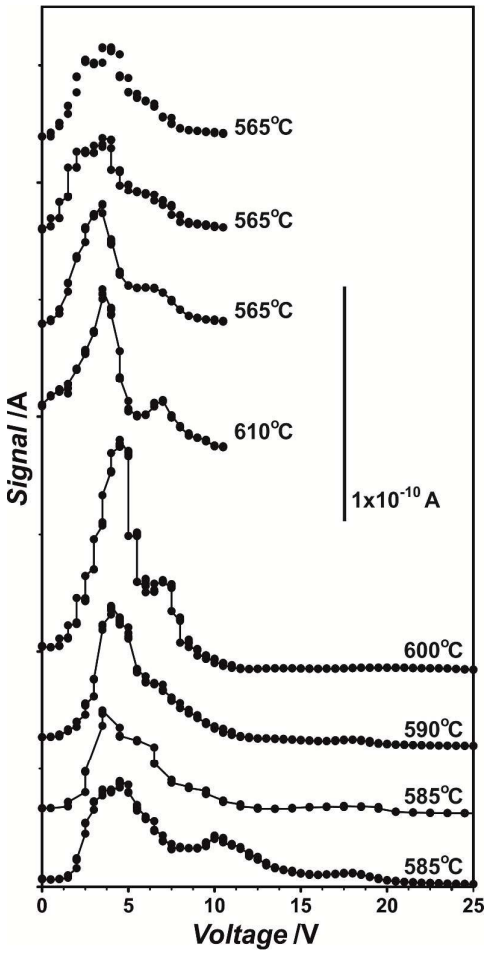

Fig. 4 Changes of the desorption signal of the excited potassium species from cryptomelane at various temperatures.

Indeed, as already mentioned, cryptomelane is considered as one of the catalytically most active phases in oxidation reactions [39].

For the measurements of Rydberg species desorption shown in Fig. 4, the sample was heated to 585°C (two consecutive measurements) after which the temperature was raised to 590, 600 and finally 610°C. After these steps the sample was cooled to 565°C for the final 3 measurements. At the beginning of the experiment, two main peaks were observed, a large peak for a sample bias between 1 and 8 V and a smaller one between 9 and 14 V. As the measurement progressed, the high voltage peak disappeared and the low voltage peak become resolved into two components, one between 1 and 5 V, and a second between 5 and 8 V.

As seen in Fig. 4, the excited K* atom signal is centred at approximately +5 V sample bias. This is also the value of sample bias used for the K atom signal, which temperature variation can be seen in Fig. 3B. At low sample voltage, the signal drops a factor of ten, and at large sample voltage, the signal vanishes. This indicates directly that the emission of excited Rydberg atoms K* is strongly increased at a few volts positive sample bias. Since the first electrode in the FID detector is at +150 V, there is no possibility that the few volts of sample bias will have any influence on the signal observed in the FID detector through the kinetic energy of the K* atoms. Thus, the action of the sample bias is local and it influences the emission process at the sample surface. Similar results have been published previously [22] from a different apparatus and another system (K on zirconia). In that case, only one sample temperature of 830°C was investigated. Thus, the features shown in Fig. 4 may be of more general meaning and not strongly dependent on the surface or the experimental details, like electric field strengths. However, a more in-depth understanding is possible here.

It is known from detailed kinetic studies of K desorption [40, 41] that the emission of K* Rydberg species depends on the crossing over to Rydberg potential energy surfaces during the desorption process from the ordinary atomic or ionic potential energy surfaces. This means that the K* emission is not in thermal equilibrium but kinetically controlled during the thermal desorption process. The crossing over to a Rydberg surface requires an electron concentration outside the surface at a distance comparable to the size of the K* Rydberg atom, of the order of 80 nm – 1 μm depending on the principal quantum number of the Rydberg atom. This quantum number is likely to be in the range n = 30 – 100, where n = 30 is the lowest quantum number for which field ionization in the FID detector is possible. Such a thermal electron cloud just outside the surface always exists at a conducting surface [38, 42]. It is due to the surface states of the electrons in the material, which exist in the relatively long-distance potential for the electrons outside the surface. The distance outside the surface over which the electrons spill out varies for example with the Fermi wavelength. This means that this distance is longer for isolators or relatively weakly conductive materials like oxides. For semiconductors the Fermi wavelength is also quite large, of the order of tens of nm as required for the formation of Rydberg species at the surface. This effect of the extension of the surface states may be the main feature that distinguishes metal surfaces (where Rydberg states are not formed) from other surfaces like oxides, where Rydberg states of alkali metals have been reported in numerous publications.

In Fig. 5 the schematic account of the electron energetics (upper part) and potassium potential energy (lower part) as a function of distance from the surface is shown. The black curves correspond to the influence of the weak electric field due to the positive bias voltage on the sample on the electron energy emitted from the Fermi level (E_F). The electron energy levels of potassium ions desorbing from the surface (shown in blue) are superimposed to illustrate the possible mutual alignment within a diabatic approximation. This figure implies that the electron outside the surface can be influenced by the external field both in energy and in distance from the actual surface. At large sample positive bias, the electron energy exceeds the ionisation potential of potassium so the electrons cannot be captured by the desorbing cations in the gas phase. At zero bias voltage, the electron emission is more efficient since the electrons are not restrained anymore. Their energy corresponds to ground state energy levels such as 4s, 4p thus such electrons can be captured transforming potassium ions into atoms as observed experimentally (Fig. 3). However, for the intermediate sample bias, at the distance where the K* are metastable (lower part of the Fig. 5 scheme) the electron energy matches the manifold of the highest energy levels of $K^+_{(g)}$. Following

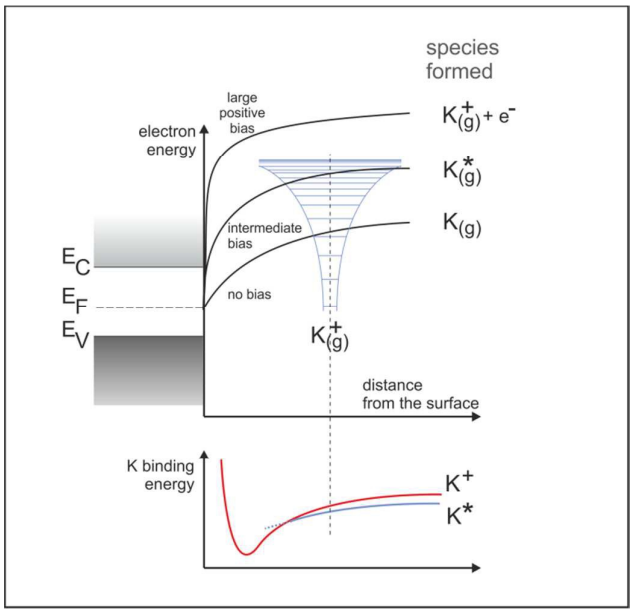

Fig. 5 Simplified energetics for the electrons in the vicinity of the surface in the presence of the weak electric field. Exponential electron energy outside the surface are superimposed with the electron energy levels of the desorbed potassium ion $K^+(g)$. Depending on the sample bias the capture of the thermal electron leads to formation of potassium atoms, ions and excited Rydberg states.

the literature [29], we may expect that when electronic motion tunes into resonance with ion desorption, energy exchange between the Rydberg electron and the ion-core becomes rapid and efficient. Below the dissociation limit of the K atom metastable Rydberg species can be formed. This simple model implies that the formation of Rydberg atoms requires not only the proper energy matching but also the electron capture at the proper distance large enough for the formation of a Rydberg atom K*. Admittedly, the figure is just a principle diagram and a quantum chemical calculation of this situation appears not straightforward at present. However, this model explains the main features of the signal variation and desorption of potassium in the form of K, K^+, K* with the applied sample bias positive voltage (Fig. 3, Fig. 4). For example, since the electronic wavefunction for the surface states in a simple one-dimensional case is exponential, it is likely that the variation with voltage should have a similar profile. The measured curves in Fig. 4 have such an approximate shape, apart from the peaks and steps in the curves.

The local peaks and steps observed in the signal at certain sample bias voltages, for example at 10 and 13 V in Fig. 4, have not been described in the literature previously. They do not appear to have fundamental importance, since they are not observed in all scans made. However, some of them are quite persistent. On a heterogeneous surface as the one studied here, several different bonding states of K and several different regions of electronic work functions exist. Each such crystallite surface may have a different distribution of the electron cloud energy and distance, and preferred location of desorption. This is likely to be the main reason for the local peak structure in the K* signal. This explanation agrees with the fact that the peak structure appears to be a function of the thermal history of the sample and thus also of the temperature as seen in Fig. 4.

As mentioned in the introductory part, cryptomelane is a very promising catalyst for the oxidation reactions. We suggest, that the activation of the reacting molecule or molecules in the vicinity of the catalyst surface may be enhanced by the presence of highly excited potassium states. This may be especially important in the cases where the contact between the catalyst and reacting substance is poor, e.g. in soot oxidation. Large radius of RM may substantially increase the number of soot particles, and the constituting molecules, influenced by the catalyst as originally proposed in [43] for organic molecules. Such chemical activation via Rydberg states may occur not only for organic molecules but also for inorganic ones as proposed in [16].

Conclusions

In conclusion, we used species resolved - thermal alkali desorption (SR-TAD) experiments to identify the potassium species leaving the surface of well-defined cryptomelane nanorods. The activation energy for K^+ ion desorption was determined to be 3.1± 0.1 eV, which is a typical value for $K–O_{surf}$ for metal oxide surfaces, whereas the K atom desorption strongly deviates from the Arrhenius energetics. We demonstrated that apart from the ionic and atomic species potassium also desorbs as a Rydberg matter. The main peak of the excited K* atom signal is centred at approximately +5 V sample bias, which is an intermediate range of the applied voltages. We postulate that the high intensity of Rydberg species for this particular voltage is caused by the match of the energy and location of the surface electrons and the energy manifold of the K^+ ions. Simple model was proposed to rationalize the speciation of potassium desorption and the observed variation of K* signal with the sample positive bias.

Acknowledgments

The research was partially carried out with the equipment purchased thanks to the financial support of the European Regional Development Fund in the framework of the Polish Innovation Economy Operational Program (contract no. POIG.02.01.00-12-023/08).

Piotr Legutko received funding for the preparation of his doctoral dissertation from the Polish National Science Center under the doctoral scholarship funding program based on the decision number DEC-2014/12/T/ST4/00687.

References

1 W. D. Mross. *Catalysis Reviews: Science and Engineering*, 1983, **25**, 17.
2 H. P. Bonzel, A. M. Bradshaw and G. Ertl, *Physics and Chemistry of Alkali Metal Adsorption*, Elsevier, Amsterdam,1989.
3 D. A. King and D. P. Woodruff, *The Chemical Physics of Solid Surfaces, Coadsorption, Promoters and Poisons*, Elsevier, Amsterdam, 1993, vol. 6.
4 J. W. Niemantsverdriet, *Spectroscopy in Catalysis*, VCH Verlagsgesellschaft, Weinheim, 1993.

5 A. Kotarba,W. Bieniasz,P. Kuśtrowski, K. Stadnicka and Z. Sojka, *Applied Catalysis A: General*, 2011, **407**, 100.
6 H. Song, H. Jiang, T. Liu, X. Liu and G. Meng, *Materials Research Bulletin*, 2007, **42**, 334.
7 I. Atribak,A. Bueno-López,A. García-García, P. Navarro, D. Frías and M. Montes, *Applied Catalysis B: Environmental*, 2010, **93**, 267.
8 G. Qiu, H. Huang, S. Dharmarathna, E. Benbow, L. Stafford and S. L. Suib, *Chemistry of Materials*, 2011, **23**, 3892.
9 P. Legutko, T. Jakubek, W. Kaspera, P. Stelmachowski, Z. Sojka and A. Kotarba, *Catalysis Communications*, 2014, **43**, 34.
10 S. L. Suib, *Journal of Materials Chemistry*, 2008, **18**, 1623.
11 A. Iyer, H. Galindo, S. Sithambaram, C. King'ondu, C.-H. Chen and S. L. Suib, *Applied Catalysis A: General*, 2010, **375**, 295.
12 G. Qiu, V.P. Santos, M.F.R. Pereira, J.J.M. Órfão and J.L. Figueiredo, *Applied Catalysis B: Environmental*, 2010, **99**, 353.
13 M. A. Peluso, L. A. Gambaro, E. Pronsato, D. Gazzoli, H. J. Thomas and J. E. Sambeth, *Catalysis Today*, 2008, **133-135**, 487.
14 L. Holmlid. *Journal of Physics: Condensed Matter*, 2002, **14**, 13469.
15 S. Ching, P. F. Driscoll, K. S. Kieltyka, M. R. Marvel and S. L. Suib, *Chemical Communications*, 2001, **23**, 2486.
16 S. Wang, H. Zheng, Q. Zhang, L. Li, H. Wu, G. Li and C. Feng, *Journal of Nanoparticle Research*, 2014, **16**, 2232.
17 A. Kotarba and L. Holmlid, Phys*ical Chemistry Chemical Physics*, 2009, **11**, 4351.
18 J. Pettersson and L. Holmlid, *Applied Surface Science*, 1989, **40**, 151.
19 S. Badiei, P. U. Andersson and L. Holmlid, *Applied Physics Letters*, 2010, **96**, 124103.
20 A. Kotarba, G. Adamski, Z. Sojka, S. Witkowski and G. Djega-Mariadassou, *Studies in Surface Science and Catalysis*, 2000, **130**, 485.
21 J. Wang and L. Holmlid, *Surface Science*, 1999, **425**, 81.
22 J. Wang, K. Engvall and L. Holmlid, *Journal of Chemical Physics*, 1999, **110**, 1212.
23 A. G. Borisov, V. Sametoglu, A. Winkelmann, A. Kubo, N. Pontius, J. Zhao, V. M. Silkin, J. P. Gauyacq, E. V. Chulkov, P. M. Echenique and H. Petek, *Physical Review Letters*, 2008, **101**, 266801.
24 J.F. Walling and A.W. Lemmon Jr., *Journal of Physical Chemistry*, 1964, **68**, 534.
25 Y. O. Dudin and A. Kuzmich, *Science*, 2012, **336**, 887.
26 S. Badiei and L. Holmlid, *Chemical Physics Letters*, 2003, **376**, 812.
27 A. Kotarba, A. Baranski, S. Hodorowicz, J. Sokołowski, A. Szytuła and L. Holmlid, *Catalysis Letters*, 2000, **67**, 129.
28 J. J. Kay, S. L. Coy, V. S. Petrović, B. M. Wong, and R. W. Field, *The Journal Of Chemical Physics*, 2008, **128**, 194301.
29 J. J. Kay, S. L. Coy, B. M. Wong, Ch. Jungen, and R. W. Field, *The Journal Of Chemical Physics*,2011, **134**, 114313.
30 B. Ura, J. Trawczyński, A. Kotarba, W. Bieniasz, M.J. Illán-Gómez, A. Bueno-López and F.E. López-Suárez, *Applied Catalysis B: Environmental*, 2011, **101**, 169.
31 K. Engvall, A. Kotarba and L. Holmlid, *Journal of Catalysis*, 1999, **181**, 256.
32 S. Dharmarathna, C.K. King'ondu, W. Pedrick, L. Pahalagedara and S.L. Suib, *Chemistry of Materials*, 2012, **24**, 705.
33 M. Sun, L. Yu, F. Ye, G. Diao, Q. Yu, Y. Zheng and J.Y. Piquemal, *Materials Letters*, 2011, **65**, 3184.
34 Y. Ding, X. Shen, S. Sithambaram, S. Gomez, R. Kumar, M.V.B. Crisostomo, S.L. Suib and M. Aindow, *Chemistry of Materials*, 2005, **17**, 5382.
35 T. Gao, M. Glerup, F. Krumeich, R. Nesper, H. Fjellvåg and P. Norby, *Journal of Physical Chemistry C*, 2008, **112**, 13134.
36 A. Kotarba, G. Adamski, Z. Sojka and G. Djega-Mariadassou, Applied Surface Science, 2000, 161, 105.
37 K. Engvall, L. Holmlid, A. Kotarba, J.B.C. Pettersson, P.G. Menon and P. Skaugset, *Applied Catalysis A: General*, 1996, **134**, 239.
38 L. Holmlid, *Zeitschrift für Physik D Atoms, Molecules and Clusters*, 1995, **34**, 199.
39 S. Dharmarathna, C.K. King'ondu, L. Pahalagedara, C.-H. Kuo, Y. Zhang and S.L. Suib, *Applied Catalysis B: Environmental*, 2014, **147**, 124.
40 M. Trebala, W. Bieniasz, L. Holmlid, M. Molenda, and A. Kotarba, *Solid State Ionics*, 2011, **192**, 664.
41 L. Holmlid, *The Journal of Physical Chemistry A*, 1998, **102**, 10636.
42 A. Zangwill, *Physics at surfaces*, Cambridge University Press, Cambridge 1988.
43 J. B. C. Pettersson and L. Holmlid, *Applied Surface Science*, 1989, **40**, 151.